Naval Research Laboratory

Washington, DC 20375-5320

NRL/MR/6120--10-9303

Interim Report on Scientific Basis for Paint Stripping: Mechanism of Methylene Chloride Based Paint Removers

JAMES H. WYNNE

Materials Chemistry Branch
Chemistry Division

KELLY E. WATSON

SAIC
Washington, D.C.

JAMES P. YESINOWSKI

Materials Chemistry Branch
Chemistry Division

CHRISTOPHER N. YOUNG
CLIVE R. CLAYTON

Stony Brook University
Stony Brook, New York

NICK NESTERUK
JACK KELLEY
TOM BRASWELL

U.S. Army Research Laboratory
Aberdeen Proving Ground, Maryland

October 18, 2010

REPORT DOCUMENTATION PAGE

Form Approved
OMB No. 0704-0188

1. REPORT DATE *(DD-MM-YYYY)*	**2. REPORT TYPE**	**3. DATES COVERED** *(From - To)*
18-10-2010	Memorandum Report	01 May 2009 - 01 May 2010

4. TITLE AND SUBTITLE

Interim Report on Scientific Basis for Paint Stripping: Mechanism of Methylene Chloride Based Paint Removers

5a. CONTRACT NUMBER

5b. GRANT NUMBER
61-9512-F0-5

5c. PROGRAM ELEMENT NUMBER

6. AUTHOR(S)

James H. Wynne, Kelly E. Watson,* James P. Yesinowski, Christopher N. Young,†
Clive R. Clayton,† Nick Nesteruk,‡ Jack Kelley,‡ and Tom Braswell‡

5d. PROJECT NUMBER

5e. TASK NUMBER

5f. WORK UNIT NUMBER

7. PERFORMING ORGANIZATION NAME(S) AND ADDRESS(ES)

Naval Research Laboratory
4555 Overlook Avenue, SW
Washington, DC 20375-5320

8. PERFORMING ORGANIZATION REPORT NUMBER

NRL/MR/6120--10-9303

9. SPONSORING / MONITORING AGENCY NAME(S) AND ADDRESS(ES)

Strategic Environment Research and Development Program
901 North Stuart Street, Suite 303
Arlington, VA 22203-1853

10. SPONSOR / MONITOR'S ACRONYM(S)

SERDP

11. SPONSOR / MONITOR'S REPORT NUMBER(S)

WP-1682

12. DISTRIBUTION / AVAILABILITY STATEMENT

Approved for public release; distribution is unlimited.

13. SUPPLEMENTARY NOTES

*Science Applications International Corporation (SAIC), 4555 Overlook Ave, SW, Bldg. 207, Room 302, Washington, DC 20375-5320
†Stony Brook University, Dept. of Materials Science and Engineering, 2275 Suny Engineering Bldg. 314, Stony Brook, NY 11794
‡U.S. Army Research Laboratory, B4600 Deer Creek Loop, Aberdeen Proving Ground, MD 21005

14. ABSTRACT

Chemical paint strippers that include methylene chloride and phenol have been extensively used to remove polymer coatings from metallic substrates. These strippers are inexpensive and remove polymeric organic coatings quickly and easily from a variety of metallic substrates without damage to the substrate. However, due to environmental and health concerns there is increasing pressure to replace methylene chloride with less hazardous alternatives. Although various alternatives to these organic solvent based systems have been developed, none equal their effectiveness in performance or cost. Thus far the mechanism of action of chemical strippers has not been adequately characterized. In order to experimentally determine the paint removal mechanisms of methylene chloride, it was important to first limit the variables in the overall process. Many of the more prominent variables exist in the coating itself, and therefore the development of simplified formulations (clear films) of each coating of interest is a logical starting point. Herein we report changes in physical and molecular-level properties of four polymer coatings upon exposure to components of the paint stripper including methylene chloride and phenol. The coatings studied were clear films of polyurethane topcoats and epoxy primers currently in military use. Using proprietary information supplied by a paint supplier, we combined the resin binders and curing agents as specified to attempt to produce clear coat films. Initial attempts failed because it was learned that the pigments and extenders provided beneficial effects in the curing process. For example, the extenders allow more expedient outgassing by providing pathways for gas to escape. To compensate for this, significant modifications to the original formula were necessary to affect flow characteristics in order to facilitate the creation of a continuous smooth film. The resultant clear coatings were characterized using differential scanning calorimetry, thermogravimetric analysis, solid state ^{1}H-nuclear magnetic resonance spectroscopy, Raman spectroscopy and attenuated total reflectance Fourier transform infrared spectroscopy.

15. SUBJECT TERMS

Paint stripper
Methylene chloride
Phenol
Polyurethane

16. SECURITY CLASSIFICATION OF:			**17. LIMITATION OF ABSTRACT**	**18. NUMBER OF PAGES**	**19a. NAME OF RESPONSIBLE PERSON**
a. REPORT	**b. ABSTRACT**	**c. THIS PAGE**			James H. Wynne
Unclassified	Unclassified	Unclassified	UL	35	**19b. TELEPHONE NUMBER** *(include area code)* (202) 404-4010

Standard Form 298 (Rev. 8-98)
Prescribed by ANSI Std. Z39.18

Table of Contents

List of Figures

List of Tables

Interim Report on Scientific Basis for Paint Stripping: Mechanism of Methylene Chloride Based Paint Removers

Background

Historically, chemical paint strippers based on methylene chloride and phenol, were widely used to remove polymeric coatings. These strippers were highly effective, inexpensive and exhibited minimal impact on the substrate. However, environmental and health concerns suggest the need for replacements. Replacement attempts have led to more environmentally friendly alternatives at the cost of performance, price and substrate damage. The mechanism by which methylene chloride and phenol work to remove polymeric coatings has not been fully characterized. This work aims to fill this knowledge gap using wet organic chemistry, solid-state proton NMR, thermal analysis and vibrational spectroscopy.

To effectively elucidate the effect of chemical paint stripper on polymeric coatings, some well characterized control polymeric coatings are needed. Commercial coatings contain not only the binder but also various pigments, fillers, flattening compounds, pigment related dispersion and wetting agents. To reduce complications from these components, this work employed control coatings made without these components. The clear films were made of five military specified coatings including three primers (MIL: 85582, 23377, and 53022) and two topcoats (MIL: 53039 and 85285).

Solid-state proton NMR shows the effects of exposure to the control solvent mixtures on the segmental dynamics of the polymer chains. It also afforded insight into the physical state of the solvent molecules of methylene chloride by indicating that the molecules were primarily in atomic-level contact with polymer molecules rather than in a larger pool of other solvent molecules. The changes as a function of temperature in the spin-lattice relaxation times (T_1), the spin-lattice relaxation times in the rotating frame ($T_{1\rho}$), and the spectra's peak widths at half-height (HHLW) after exposure to methylene chloride or phenol/water solutions are reported. Studies were done as a function of temperature to allow for comparison between dynamics induced from solvent exposure and those induced solely by increasing temperature.

Thermal analysis of the coatings before and after exposure to control solvent mixtures of individual components typically found in commercial paint stripper can give insight into the

Manuscript approved September 13, 2010.

degradation caused by the paint stripper. By studying the change in glass transition temperature the specific solvent mixtures that were responsible for significant degradation of the coatings have been identified. Differential Scanning Calorimetry (DSC) scans taken of coatings after exposure to the control solvent mixtures show decreases of the glass transition temperature by as much as 100 ^{0}C. Changes in the Thermogravimetric Analysis (TGA) curve can also illustrate a solvent mixture's activity and suggest both the physical and chemical degradation mechanism. One can attempt to mimic the effects using different solvents to verify the active functional groups. Vibrational spectra of the coatings obtained before and after exposure showed changes in the coating's structure.

Materials and Methods

Chemicals

All chemicals were reagent grade and used without further purification. Mixtures were prepared by weight according to ratios depicted in Table 1.

Table 1. List of the composition of the control solvent formulations.

		Weight Percent			
Solution		methylene chloride	ethanol	water	phenol
	Commercial paint stripper[a]	60.6	5.8	7.8	15.8
	Methylene chloride	100	---	---	---
	Methylene chloride and ethanol	91	9	---	---
	Methylene chloride, ethanol and water[b]	82	8	10	---
	Methylene chloride, ethanol, water and phenol[b]	67	6	9	18
	Phenol and methylene chloride	79	---	---	21
	Phenol and ethanol	---	27	---	73

[a]Also contains Methocel (1.2%), toluene (1.3%), sodium petroleum sulfonate (5.5%) and paraffin wax (1.9%), [b] Methocel added to emulsify into a single phase.

Coatings

Currently employed military coatings were selected for this study. These included two polyurethane topcoats and two epoxy primers. The coatings were unsupported (free films) with a film thickness of approximately five mils, see Table 2, of four military coatings; MIL-PRF-23377, MIL-PRF-85582, MIL-DTL-53039, MIL-PRF-85285.

Table 2. Current military coatings studied.

Military Specification	Final thickness (mm)	Specific coating description
MIL-DTL-53039	0.13	Single Component Aliphatic Polyurethane CARC Topcoat
MIL-PRF-85285	0.13	Two Component High Solids 2.8 VOC Polyurethane Topcoat
MIL-PRF-23377	0.13	Two component Chromated Epoxy Polyamide Epoxy Primer
MIL-PRF-85582	0.17	One component Waterborne Chromated Epoxy Primer

Complete coating formulations can be found in Tables 3-6. The simplification of the otherwise complex coating system was selected to allow for ease of analysis. Resin binders and curing agents were combined as specified in Tables 7-10 to produce clear coat films of the selected four military coatings. Each clear coat formulation was produced without pigments, additives, and solvents. In order to cast clear formulations to the required film thickness it was necessary to compound formulas to a workable spray application viscosity by adding the solvents contained in each formula in the proportions and thinning ratios specified. Elimination of entrapped air or solvents required either the addition of an antifoam agent or the readjustment of antifoam agent amounts or both. Antifoam agents used were those normally contained in each formula and were added in the proportions specified in Tables 7-10.

Complete Coating Formulations:

Table 3. MIL-PRF-23377 Epoxy Polyamide Primer.

Part A Raw Material	Wt %	**Part B** Raw Material	Wt %
Acetone	12	Acetone	0.7
2,4,6-Tri (dimethylaminomethyl) phenol	0.5	Methyl *N*-amyl ketone	1
Fatty aminoamide	1	Dimethyl glutrate & succinate	1.2
Butyl urea formaldehyde	2.2	Epoxy resin	14.7
Polyamid resin	7		
Dispersion agent	0.2		
Silica gel	3		
Ceramic microspheres	3		
Titanium dioxide	6.5		
Extender pigment	47		

Table 4. MIL-DTL-53039 Single Component Aliphatic Polyurethane CARC.

Raw Material	Wt %	Raw Material	Wt %
Polyurethane	31	Cobalt titanate spinel	0.4
Dispersant	1	Methyl isoamyl ketone	23.5
Rheology modifier	0.1	VM&P naptha	3.2
Flow modifier	<0.1	Xylene	1.4
Surfactant	0.1	*n*-Butyl acetate	1.3
Dibutyl tin dilaurate	0.5	Aromatic 100	1.3
Celite	18.5	Mineral spirits	1.2
Imsil	3.6	Propylene glycol	0.1
TiO_2	9.5	Isobutyl ketone	0.1
Iron oxide hydrate	2.5	*n*-Butyl acid phosphate	0.1
Carbazole dioxazine violet	<0.1	Bentone	0.5

Table 5. MIL-PRF-85285 High Solids Polyurethane Topcoat.

Part A Raw Material	Wt %	**Part B** Raw Material	Wt %
Methyl *N*-propyl ketone	1	Polyurethane resin	43
Methyl *N*-amyl ketone	7	*N*-Butyl acetate	1.6
Anti-oxidant	0.3		
UV-absorber	0.5		
UV stabilizer	1		
Polyester solution #1	19.3		
Cellosolve acetyl butyrate	0.6		
Surfactant	0.1		
1% Thickener in xylene	0.2		
Thixotropic agent	0.2		
Dispersing agent	0.3		
TiO_2	20.5		
Polyester solution #2	4.4		

Table 6. MIL-PRF-85582 Waterborne Epoxy Primer.

Part A Raw Material	Wt %	**Part B** Raw Material	Wt %
2-Propanol	1.8	Epoxy resin	17
2-Propoxyethanol EP	4	Bisphenol A epichorohydrate	20
Glycol ether DPNB	1	Deionized water	6.8
Acetone	3		
Triaminosilane	1.2		
Non-ionic acrylic copolymer	0.3		
Polyamine curing agent	1.2		
Amine functional emulsion	18.1		
Modified aliphatic amine	1.2		
Natural silica	6		
Silica 10 micron	6		
Magnesium silicate-flakey	2.4		
TiO_2	2.7		
Aqueous carbon black dispersion	<0.1		
Strontium chromate	7.3		

Clearcoat Formulations:

Table 7. 23377 Epoxy Polyamide Primer Type Clearcoat.

Part A	Wt %	**Part B**	Wt %
Polyamid resin	19.2	Epoxy resin	41.2
Fatty aminoamide	2.8	Methyl N-amyl ketone	2.8
Butyl urea formaldehyde	6.2	Acetone	5.9
Acetone	20	Dimethyl glutarate & succinate	1.2
2,4,6-Tri(dimethylaminomethyl) phenol	0.5		
Dispersant	0.2		

Table 8. 53039 Single Component Aliphatic Polyurethane CARC Clearcoat.

Raw Material	Wt %
Polyurethane	47.4
Dibutyl tin laurate	0.7
Dispersant	0.1
n-Butyl acetate	2
Methyl isoamyl ketone	38.2
Surfactant	0.2
Flow modifier	0.1
Rheology modifier	<0.1
VM&P naptha	4.8
Xylene	2.1
Aromatic 100	2
Mineral spirits	2
Propylene glycol	0.0
Isobutyl ketone	0.2
n-Butyl acid phosphate	0.2

Table 9. 85285 High Solids Polyurethane Topcoat Type Clearcoat.

Part A Raw Material	Wt %	**Part B** Raw Material	Wt %
Polyester solution #1	24.4	Polyurethane resin	54.4
Polyester solution #2	5.5	*N*-Butyl acetate	2
Methyl *N*-amyl ketone	8.9		
Methyl *N*-propyl ketone	1.3		
Anti-oxidant	0.4		
UV absorber	0.6		
UV Stabilizer	1.3		
Cellosolve acetyl butyrate	0.8		
Surfactant	0.2		
1% Thickener in xylene	0.2		

Table 10. 85582 Waterborne Epoxy Primer Type Clearcoat.

Part A Raw Material	Wt %	**Part B** Raw Material	Wt %
Amine emulsion	24	Epoxy resin	22.1
Anquamine	1.5	Bisphenol A epichorohydrate	26
Curing agent	1.5	Deionized water	5
2-Propanol	2	Antifoam	1
2-Propoxyethanol EP	5		
Glycol ether DPNB	1		
Acetone	4		
Triaminosilane	1.5		
Non-ionic acrylic copolymer	0.4		

The formulas were compounded to achieve continuous, anomaly-free films of the desired thickness by utilizing the identical rheology and flow modifiers specified in each formula. Clear films were created by spray application after altering the proportions of solvents, adhesion promoters, antifoamers, rheology, and flow modifiers utilized in each clear coating formulation as necessary. Initial application using conventional spray equipment failed due to the high viscosity of the formulations. A drawdown mechanism of application for creating coatings also failed as creating films of the approximate four mils thickness in a single application trapped gas and formed bubbles upon curing. For the material to cure properly to achieve the required film thicknesses, it was necessary to apply multiple film layers, allowing each to cure before applying another layer. This was crucial to avoid solvent entrapment and the resulting complications. All formulations were sprayed in multiple layers on release paper allowing 16-24 hour cure time between each layer and a final seven day cure time. This minimized bubble formation and created coatings of the desired thickness. All clear coatings were prepared on release paper.

Sample Exposure

For thermal analysis the samples were exposed as follows. Approximately two centimeter square coupons of each coating were cut and placed into individual scintillation vials. To each vial was added the respective solvent or solvent mixture (see Table 1) until the coating was completely covered (~10 mL). After exposure periods of two hours and two days, respectively, the liquid was decanted, rinsed with absolute ethanol and the coating allowed to air dry in the vial. A rinse with ethanol ensured that no remaining chemicals were adhered to the surface of the coating prior to analysis. Caution was taken to ensure the coating was completely dry before testing.

For Raman Spectroscopy the samples were exposed for times ranging from 15 minutes to two hours. The samples were then air dried thoroughly, for times ranging from two hours to two weeks, to reduce spectral contamination from residual solvent. Solvents systems used included liquid phenol (89:11 phenol/water) as well as a selection of the solvent mixtures listed in Table 1.

Differential Scanning Calorimetry (DSC)

Differential scanning calorimetry (DSC) was performed on a TA Instruments Q20 DSC with the DSC Refrigerated Cooling System (RCS) and a purge gas of nitrogen set to 50 mL/min. Samples of approximately 1-2 mg were placed into TA Instrument Tzero Aluminum pans and an empty aluminum pan was used as reference. Samples were analyzed from -90 °C to 150 °C at 20 °C/min twice to demonstrate hysteresis. All data reported were taken from the second cycle. Glass transition temperatures (T_g)were found using TA Universal Analysis program.

Thermogravimetric Analysis (TGA)

Thermogravimetric analysis (TGA) was performed on a TA Instruments Q50 TGA using a platinum sample pan. The analysis was carried out in the presence of oxygen with breathing air used as the sample purge gas. Nitrogen was used as the purge gas for the balance. Data were recorded from ambient temperature to 700 °C at a 5 °C/min ramp. Plots of percent weight loss versus temperature were constructed to analyze the data.

Fourier Transformed Infrared Spectroscopy-Attenuated Total Reflectance (FTIR-ATR)

FTIR spectra were recorded on a Thermo Scientific Nicolet 6700 FTIR spectrometer equipped with a Smart Performer ATR attachment with a germanium crystal at 432scans. Spectra were recorded from 4000 – 500 cm^{-1} with a resolution of 2 cm^{-1}, and were analyzed using the Nicolet OMNIC software suite.

Raman Spectrometry

Samples were analyzed using either a Nicolet Almega dispersive Raman spectrometer with 10x objective lens and 785 nm or 532 nm excitation laser; or a WiTec Alpha 500 confocal Raman

spectrometer with 20x objective and 532 nm laser, at Brookhaven National Laboratory's Center for Functional Nanomaterials; the spot sizes on these instruments are less than 3 μm.

Gas Chromatography – Mass Spectrometry (GC-MS)

The GC-MS system was an Agilent 7890A gas chromatograph equipped with an Agilent 5975C mass selective detector operating in electron ionization mode and an Agilent 7693A autoinjector. The column utilized was an Agilent HP-5MS (5 % phenyl) methylpolysiloxane film. The carrier gas was helium with a flow rate of 1 mL/min^{-1}. The injection temperature, MS quadrapole temperature, and source temperature were 250 ºC, 150 ºC and 230 ºC, respectively. The detector was set to scan with a mass range of 15 to 250 *m/z*. The temperature program has an initial temperature of 35 ºC for one minute, then 0.5 ºC per minute ramp to 37 ºC followed by a 5 ºC per minute ramp to 80 ºC and then a 20 ºC per minute ramp to 110 ºC with a two minute post run hold at 250 ºC.

Proton (^{1}H) Solid State NMR

The ^{1}H NMR spectra and ^{1}H relaxation times were obtained at 500 MHz (11.7 T field) on a Bruker Avance DMX-500 NMR spectrometer. Measurements of the spectra yielding a full-linewidth at half-height (HHLW), the spin-lattice relaxation time (T_1) and the spin-lattice relaxation time in the rotating frame ($T_{1\rho}$) were made as a function of temperature to allow comparison of the dynamics induced by an increased temperature with dynamics induced by solvent activity. ^{1}H NMR studies were done on MIL-53039 before and after a five minute room-temperature exposure to methylene chloride and on MIL-23377 before and after a ten minute room-temperature exposure to a phenol:ethanol (2.724:1 weight ratio) solution.

The ^{1}H spin-lattice relaxation times T_1 were measured using a saturation-recovery pulse sequence with typically a dozen different recovery delays, and fitting the recovery curve of the peak intensity using OriginPro 7.0 to a single-exponential recovery curve with time constant T_1. The intensities of static ^{1}H NMR peaks vs. spin-lock times (typically nine values) in a spin-locking pulse sequence were fit using Origin to a single-exponential decay curve with a decay time constant $T_{1\rho}$. Measurements (Figure 1) were repeated at different temperatures and for different samples.

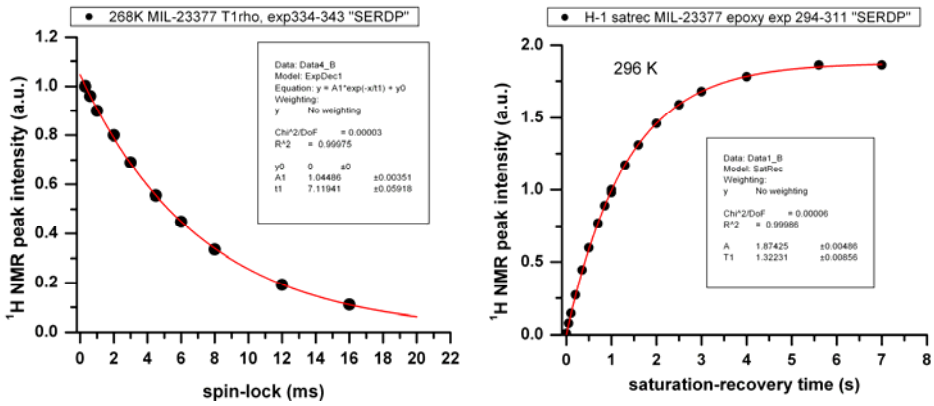

Figure 1. Examples of $T_{1\rho}$ and T_1 data analysis each for one sample at one temperature.

Results and Discussion

Commercial paint remover (MIL-R-81294) was purchased and analyzed utilizing a rapid separation of volatiles followed by GC-MS analysis. The presence of methylene chloride (CH_2Cl_2), toluene, ethanol (EtOH), phenol (PhOH) and water were all confirmed; however, the content of each differed as much as 8% from the reported values in Table 1. This was not surprising due to variability in batch manufacture as well as the possibility of chemical reactivity within the can. Additionally, it should be noted that the utility of thickeners and other surfactants could also contribute to the resulting low values for some of the more reactive volatiles. This is expected as outlined in Figure 2 below, confirming metathesis of the proton of phenol with the sulfonate salt can readily occur.

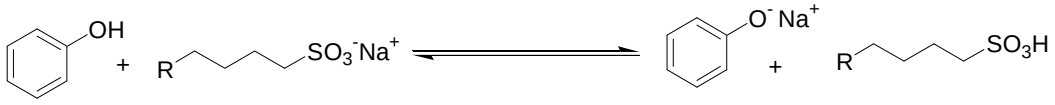

Figure 2. Chemical equilibrium illustration.

The types of resin binders, curing agents, pigments, and additives chosen by a coatings formulator are specifically selected to perform a particular set of functions depending on the performance specifications of the completed coating. The resin/binder and pigment system chosen for a primer is not the best system for a topcoat. The intent in the creation of simplified films was to retain the resin and curing agent ratios while eliminating the pigment portion of the coating to produce clear films of a specified thickness, unsupported or free-standing, for testing purposes.

The removal or change in the amount of one ingredient will in all probability affect the performance characteristics of the coating. In the case of pigment removal from a coating, the effect can be catastrophic, much like what would happen if the reinforcements and aggregate were removed from the concrete used in construction. Because they are chemically different, each coating has required major reformulation measures just to form a continuous, uniformly cured film. The various types of coatings and binder types made each of the five coatings a unique challenge.

The biggest challenge was to create 4 mils dry film thickness (DFT) films by applying the clear coatings over a film releasing type substrate utilizing a Byrd applicator. Combining only the resin and curing agent (where applicable) components of the formulas resulted in very thick pasty mixtures that failed to form defect-free films of the uniform thickness required. While thin enough to apply with an adjustable Byrd applicator, films would not release intact from the glass substrate, and “crawled” when applied to plastic coated butcher’s paper, waxed paper, and Teflon substrates, forming discontinuous films of varying DFT. Successful release was facilitated using the aircraft release paper, but an even thickness could not be obtained using the drawdown method due to the paper wrinkling under the pressure of the Byrd applicator, and failure of the films to level into a uniform wet film thickness (WFT). In all cases the resin combinations alone were much too viscous to apply with conventional spray equipment. Therefore significant modifications were made to the initial plan.

First, changes were required in the casting of the clear formulations to the required film thickness. Problems were encountered because making a thicker drawdown of the clear material within a WFT range of 10 to 20 mils of a coating that is normally pigmented and designed to be sprayed in much thinner WFT applications ranging from 1 to 2.5 mils creates radically different flow, wetting, curing, and surface tension properties. Attempts at casting the clear formulas were designed to utilize the greater weight of a thick film to overcome surface tension between the substrate and the clear coating, theoretically allowing a continuous, uniformly thick film to form. It was necessary for small amounts of solvent to be added to facilitate better flow and leveling. In the polyurethane formulas, carbon dioxide bubbles evolved during the curing reaction remained trapped in the film. Further thinning of these formulas, while ridding the film of most entrapped bubbles, didn’t prevent bubbles from forming on the surface. The curing of an initially clear

polyurethane film would develop into a hazy, bubble entrapped film overnight due to reaction with moisture in the atmosphere. The epoxy clear coatings would only partially cure at the higher casting thicknesses as entrapped solvents were probably preventing complete curing of the film. These films were cloudy looking and remained soft and pliable.

Second, changes were made to the compound formulas by adding the solvents contained in each particular formula in the proportions and thinning ratios specified in order to achieve a workable spray application viscosity. Thinning with solvent blends proportional to amounts specified in each formula was necessary to reduce these formulas to a spray-apply viscosity. Retaining each specific formula's solvent blend ratio was done to not only reduce formulation variables, but to also minimize the possible impact of varying solvent evaporation rates on curing properties and film formation. Evaporation actions of solvents may cause the formation of Bénard cells, causing noticeable film imperfections (Figure 3). With thinner films surface tension forces become more crucial.

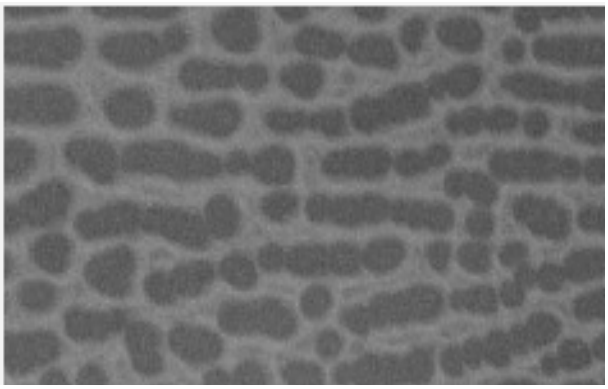

Figure 3. Bénard Cells induced by solvent evaporation due to vortex circulation and change in viscosity.[i]

Third, changes were made to eliminate entrapped carbon dioxide and air by the addition of antifoam agents contained in each formula in the proportions specified. Pigments tend to affect surface tension for the better in flat coatings, almost acting as stabilizers, even aiding in bursting bubbles through surface tension means and physically bursting them, like a pin popping a balloon. When pigments are removed, surface tension force effects are often increased, particularly in high gloss coatings and clears resulting in trapped bubbles (Figure 4). Designed to modify a coating's surface tension, including in some cases through the addition of fumed silica to act as tiny glass shards to physically burst the bubble, antifoaming agents utilized in the

proper amount will prevent the formation of bubbles on the coating's surface. Too much antifoam additive, or the wrong type, can cause cratering, adhesion problems, and color acceptance problems. Where necessary and when included in the original formulation, anti-foaming agents were retained in the clear formulations and adjusted accordingly.

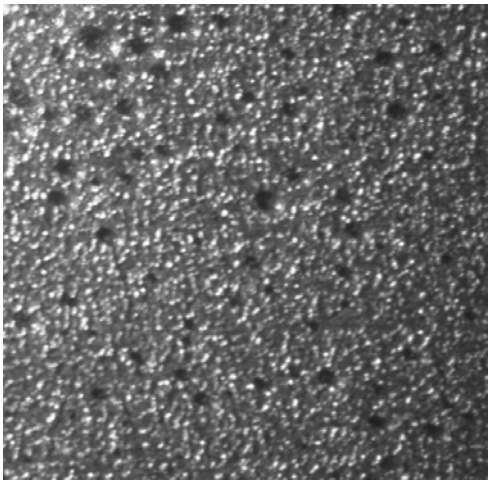

Figure 4. Trapped gas shown in early attempts at clear film application on a chromate aluminum substrate.

Fourth, changes were made to compound formulas to achieve continuous, anomaly-free films of the required thickness requested by utilizing the identical rheology and flow modifiers specified in each formula. Due to the removal of pigments from all formulas, modification of flow characteristics to facilitate the creation of a continuous smooth film of optimal DFT was necessary. Substrate adherence additives and flow modifiers were the key to creating defect-free films (Figures 5).

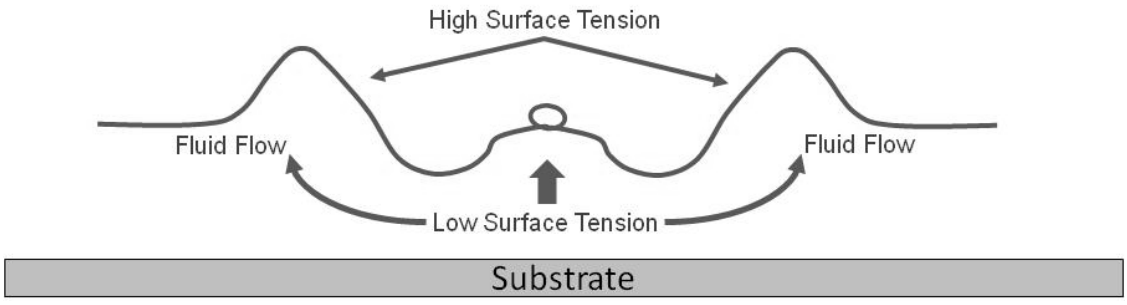

Figure 5. Fisheye and cratering defects due to surface tension differences between the substrate and the coating's top surface.

An example of the effects of a flow modifier on coating film quality is shown in Figure 6. Determination of the right amount of any additive to obtain optimal flow and leveling characteristics is critical.

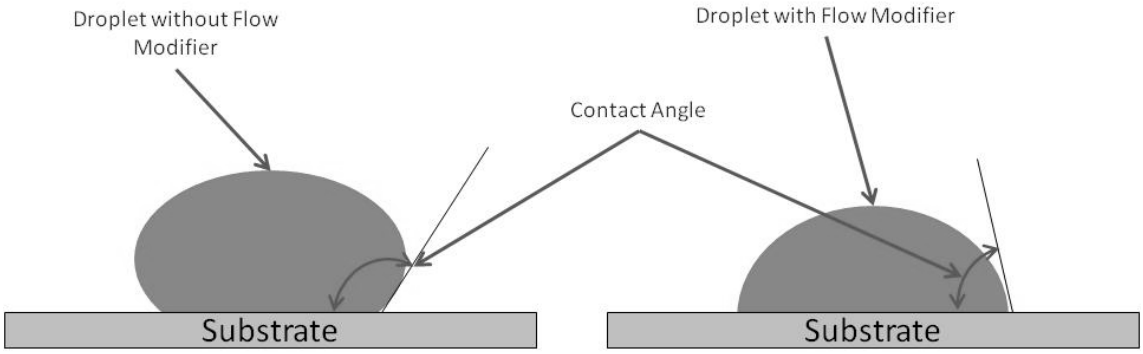

Figure 6. Illustration of how flow modifiers aid in the wetting of the substrate by reducing surface tension.

Fifth, the required clear films were created by spray application rather than by drawdown which was the original plan. Clear films were created after altering the proportions of solvents, adhesion promoters, antifoamers, rheology, and flow modifiers utilized in each clear coating formulation as necessary. Building up the film thickness by spraying multiple coats until achieving the DFT required, though an extremely lengthy process, was the only way to provide the DFT and quality specified. This proved to be the most successful method because it facilitated the application of WFT more in line with the intended design of the original formulation. For the material to cure properly to achieve the required film thicknesses, it was necessary to apply multiple film layers, allowing each to cure before applying another layer. This was crucial to avoid solvent entrapment and the resulting complications.

Samples of fully formulated chemical agent resistant coating (CARC) paint as well as Air Force topcoat were prepared on release paper and characterized for baseline measurements using Fourier transformed infrared spectroscopy - attenuated total reflectance (FTIR-ATR), thermogravimetric analysis (TGA), differential scanning calorimetry (DSC) and dynamic mechanical analysis (DMA). The purpose of this preliminary study was to determine that the method and instrumental technique was not only compatible with the individual instrument, but also to determine that the sample thickness was sufficient to perform under the specified method once the control formulation coatings became available. Additionally, special containment was

designed to ensure that the DMA could function in a methylene chloride environment, which involved changing the o-rings to a more solvent resistant system.

Upon receiving the clear control films, characterization by FTIR-ATR ensured the correct functionalities were present as well as to provide a snapshot as to the degree of curing by examining free unreacted functional groups. After observing satisfactory results, TGA analysis was performed to ensure the absence of nontraditional species such as inorganic additives. All coatings demonstrated less than 1 % by weight incombustible material in a breathing air atmosphere, which was acceptable for subsequent analyses.

In an attempt to find evidence of chemical and physical changes, DSC was employed on each of the coatings upon exposure to controlled combinations of the depaint ingredients as seen in Table 11. This was followed by analysis of the exposed coating using TGA. The control solutions of phenol (PhOH) with methylene chloride and separately with ethanol (EtOH) were tested for the effect on the coatings after observation of the significant change to the coatings exposed to the mixture containing phenol. DSC was performed on all exposed coatings while TGA was only performed on coatings exposed to solvent for two hours. The solutions used for thermal studies are shown in Table 1.

Table 11. Reported T_g values from DSC.

		MIL-DTL-53039	MIL-PRF-85285	MIL-PRF-85582	MIL-PRF-23377
Control		100	51	62	40
2 hour exposure	CH_2Cl_2	67	46	74	49
	CH_2Cl_2 & EtOH	67	44	76	48
	CH_2Cl_2, EtOH & Water	70	45	77	48
	CH_2Cl_2, EtOH, Water & PhOH	-11	decomp	decomp	17
	CH_2Cl_2 & PhOH	-4	-30	-18	-22
	EtOH & PhOH	-9	-25	-33	-19
Two day exposure	CH_2Cl_2	72	44	70	51
	CH_2Cl_2 & EtOH	65	41	76	49
	CH_2Cl_2, EtOH & Water	70	43	82	51
	CH_2Cl_2, EtOH, Water & PhOH	-4	decomp	decomp	-5

Attempts to identify the specific chemical changes within the coating employed FTIR-ATR. Additionally, the use of dynamic mechanical analysis would also be beneficial; however, the

current primer systems are too brittle and the polyurethane coatings are not thick enough to allow for adequate clamping without breakage or slippage. Attempts to adhere other substrates to facilitate dampening resulted in the generation of irreproducible tan-delta measurements.

For coating MIL-DTL-53039, the one-component CARC polyurethane, DSC shows a glass transition temperature (T_g) of 100 °C for the control coating; however, the T_g was at 66 °C after a two hour exposure to methylene chloride and at 72 °C after a 4 day exposure. The T_g was 67 °C and 65 °C when exposed to methylene chloride and EtOH for two hours and two days respectively. Exposure to methylene chloride, EtOH and water for two hours and for two days affords a T_g of 70 °C. These temperatures are basically equivalent when considering the standard error of the instrument. Exposure to the methylene chloride, EtOH, water and PhOH solution for two hours decreases the T_g of the coating to -11 °C and exposure for two days decreases it to -4 °C, while exposure to methylene chloride and PhOH decreases the T_g to -4 °C. Exposure to EtOH and PhOH decreases the T_g to -9 °C. It was also noted that exposure to EtOH and PhOH caused the coating to separate into two layers with different physical properties, although each layer had similar T_g values. Exposure to methylene chloride and PhOH results in the onset of delamination; however, no other solvent causes such separation, making it unreasonable to assume that the separation results from film preparation. The TGA for MIL-DTL-53039 both before and after exposure can be seen in Figure 7. The TGA of the coatings exposed to mixtures without PhOH are all similar to that of methylene chloride alone. All of these mimic the shape of the TGA control coating except a larger weight loss by 150 °C. The TGA of the coatings exposed to PhOH containing mixtures show immediate weight loss and a different graph shape including a more severe (~50%) weight loss by 200 °C. Measurement of the TGA of the PhOH and EtOH exposed coating was preempted by the coating's separation into two layers.

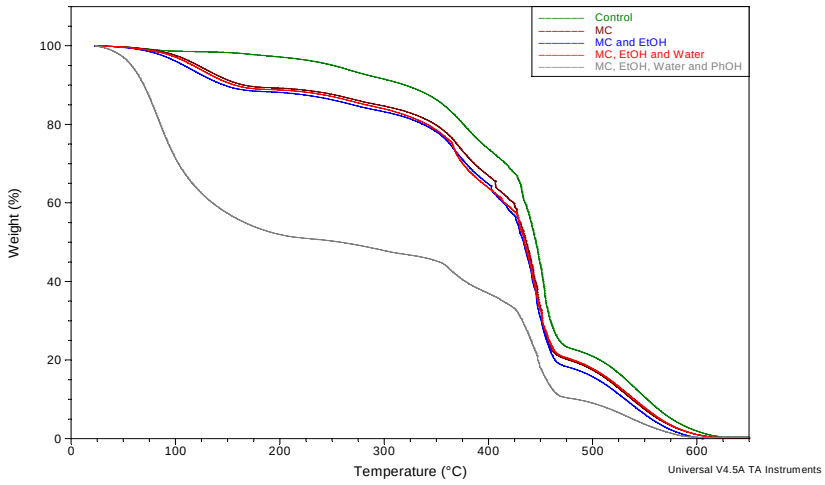

Figure 7. TGA overlay for CARC polyurethane (MIL-53039).

For coating MIL-PRF-85285, the two-component polyurethane NAVY topcoat, DSC showed a T_g of 50 °C; however, it dropped slightly to 46 °C after a two hour exposure and to 44 °C after the 4 day exposure to methylene chloride. The T_g was 44 °C and 41 °C when exposed to methylene chloride and EtOH for two hours and two days, respectively. Exposure to methylene chloride, EtOH and water for two hours gives a T_g of 45 °C and exposure for two days affords a T_g of 41 °C. These temperatures are equivalent when considering the standard error of the instrument. The sample of this coating that was exposed to methylene chloride, EtOH, water and PhOH however, decomposed into small pieces preventing DSC or TGA analyses. Exposure to methylene chloride and PhOH decreases the T_g to -30 °C, while exposure to EtOH and PhOH decreases the T_g to -25 °C. The TGA results for this coating (MIL-PRF-85285) can be seen in Figure 8. They follow the same patterns as the TGAs of MIL-DTL-53039.

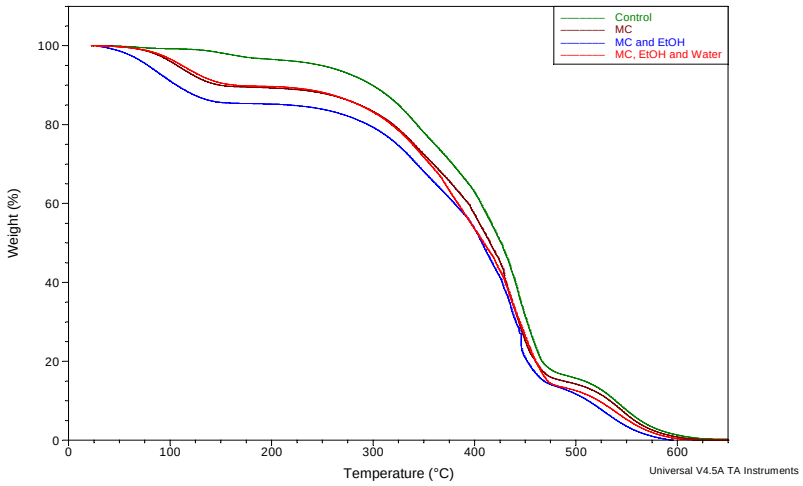

Figure 8a. TGA overlay for NAVY topcoat polyurethane (MIL-85285).

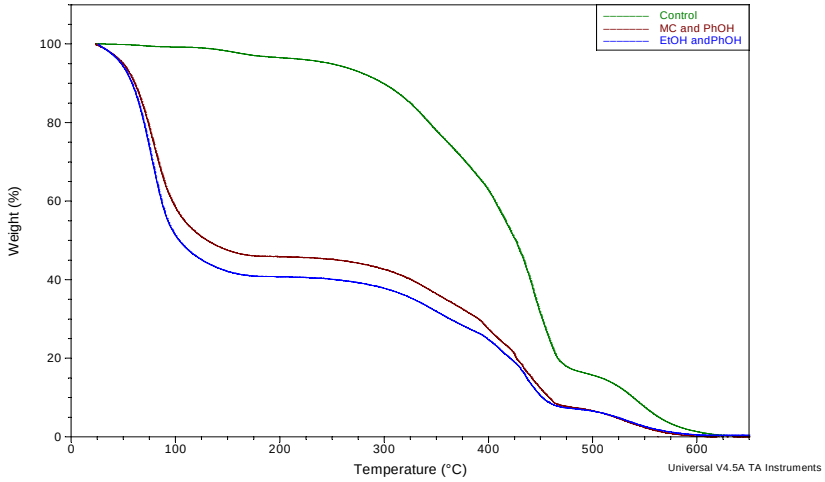

Figure 8b. TGA overlay for NAVY topcoat polyurethane (MIL-85285).

For coating MIL-PRF-85582, the water-borne epoxy primer, DSC shows a T_g of 62 °C for the control coating. It shows a T_g of 74 °C after two hour exposure and 70 °C after the two day exposure to methylene chloride. The T_g was 76 °C when exposed to methylene chloride and EtOH for two hours and two days. Exposure to methylene chloride, EtOH and water for two hours gave a T_g of 77 °C and exposure for two days afforded a T_g of 82 °C. The temperatures are all approximately equivalent when considering the standard error of the instrument. The sample of this coating that was exposed to methylene chloride, EtOH, water and PhOH decomposed into small pieces, like MIL-85285, preventing DSC and TGA analysis. Exposure to methylene chloride and PhOH decreases the T_g to -18 °C. Exposure to EtOH and PhOH

decreases the T_g to -33 °C. The TGA of the MIL-85582 coatings can be seen in Figure 9. Those exposed to mixtures without PhOH mimic the shape of the TGA of the control coating except for a weight loss that is slightly greater than the control which occurs by 200 °C. Comparing solvents, exposure to methylene chloride alone causes the smallest amount of this initial weight loss, while the methylene chloride, EtOH and water exposure causes the greatest amount of weight loss. TGA of the coatings exposed to the PhOH containing two component mixtures shows near immediate weight loss and a different graph shape. This includes a more severe weight loss, 50 % and 70 % by 200 °C, with the EtOH and PhOH mixture showing the greater weight loss.

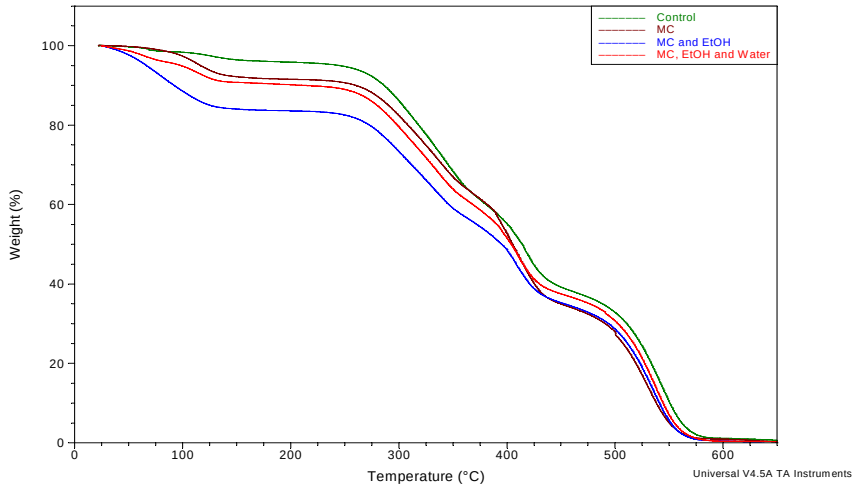

Figure 9a. TGA overlay for Waterborne Epoxy Primer (MIL-85582).

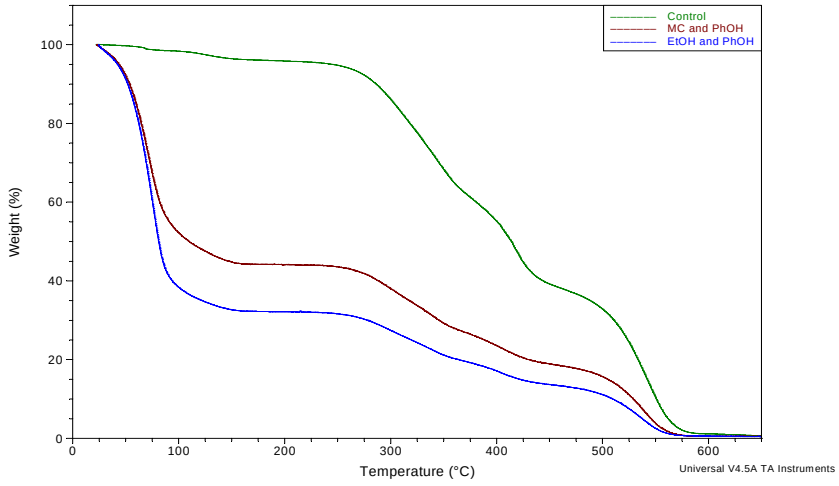

Figure 9b. TGA overlay for Waterborne Epoxy Primer (MIL-85582).

For MIL-PRF-23377, the two-component solvent-borne epoxy primer, DSC shows a T_g of 40 °C for the control. The T_g was 48 °C and 49 °C when exposed to methylene chloride and EtOH for two hours and two days, respectively. Exposure to methylene chloride, EtOH and water for two hours gives a T_g of 48 °C and exposure for two days gives one of 51 °C. These temperatures are all equivalent when considering the standard error of the instrument. It appears that the analysis process is most likely resulting in additional crosslinking of the already highly crosslinked system. Exposure to the methylene chloride, EtOH, water and PhOH solution for two hours decreases the T_g of the coating to 17 °C and exposure for two days decreases it to -5 °C. Exposure to methylene chloride and PhOH decreases the T_g to -22 °C. Exposure to EtOH and PhOH decreases the T_g to -19 °C. The TGA of the MIL-23377 coatings can be seen in Figure 10. Those exposed to mixtures without PhOH mimic the shape of the TGA of the control coating. The methylene chloride/EtOH mixture and methylene chloride only exposure cause a weight loss greater than the control by 150 °C, with the former being more severe. The TGA of the coatings exposed to PhOH containing mixtures show near immediate weight loss and a different graph shape including a more severe (~50%) weight loss by 200 °C.

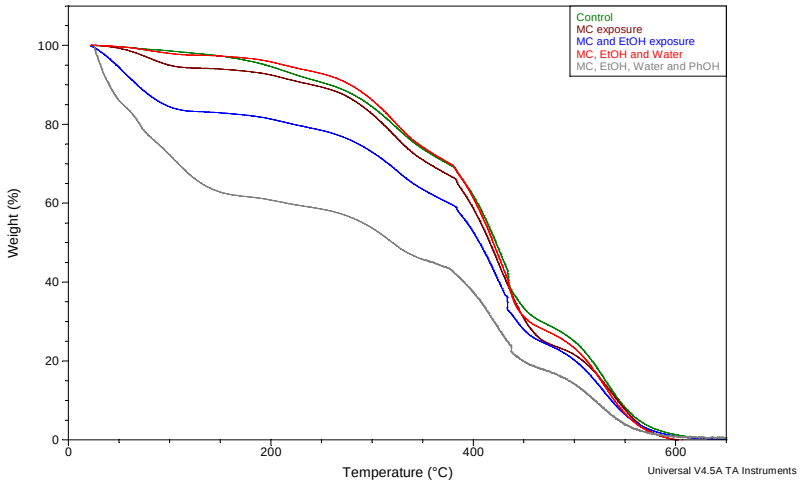

Figure 10. TGA overlay for Polyamide Epoxy Primer (MIL-23377).

It was noted, some weeks after testing the samples, that coatings which had been exposed to a solvent mixture containing phenol exhibited a color change. The original coating samples are clear or slightly opaque. MIL-DTL-53039 and MIL-PRF-85285 turn a pink color after exposure to phenol while MIL-PRF-85582 and MIL-PRF-23377 turn an orange color. Figure 11 shows an example of the color change. The pink coating on the left is MIL-DTL-53039 (the CARC

polyurethane topcoat) after exposure to methylene chloride, ethanol, water and phenol. The orange coating on the right in Figure 11 is MIL-PRF-23377 (the polyamide epoxy primer) after exposure to methylene chloride and phenol.

Figure 11. Examples of coating's color change after exposure.

In order to create a mechanistic model the chemical changes induced by solvents drawn from the paint stripper were evaluated using Raman and FTIR spectroscopic analyses. FTIR and Raman spectra have been obtained for each sample before and after exposure to the selected solvent mixtures. In this report, results obtained from system 53039 will be presented.

Figure 12 shows the Raman spectra of MIL-53039 before and after exposure to methylene chloride and EtOH (82:8) as well as a magnified view of the carbonyl region of the spectrum at 1747 cm^{-1}. Several extra peaks are visible; these correspond to components of the solvents applied. Here, methylene chloride and ethanol are detected readily within the sample, even after extended periods of drying. Considering the comparatively short exposure time of the analyzed sample (15 minutes) as compared to drying time (two hours), the significant presence of solvent components within the coating must be indicative of considerable solvent entrapment by the resin matrix. Of particular interest in the spectra shown is a minor height decrease and shift in the carbonyl (C=O) peak at 1747 cm^{-1}, as a result of exposure to solvents containing methylene chloride; there is a broadening and shift of approximately 2 cm^{-1}. This indicates a minor dilation of the hydrogen bonds between the polyurethane chains (C=O---H-N), supporting the notion that methylene chloride acts to facilitate penetration by larger solvent molecules though matrix swelling/dilation. Complementary data collected by FTIR supports this conclusion. In the FTIR spectrum there is a minor peak decrease at 1683 cm^{-1}, corresponding to the infrared-active C=O vibration.

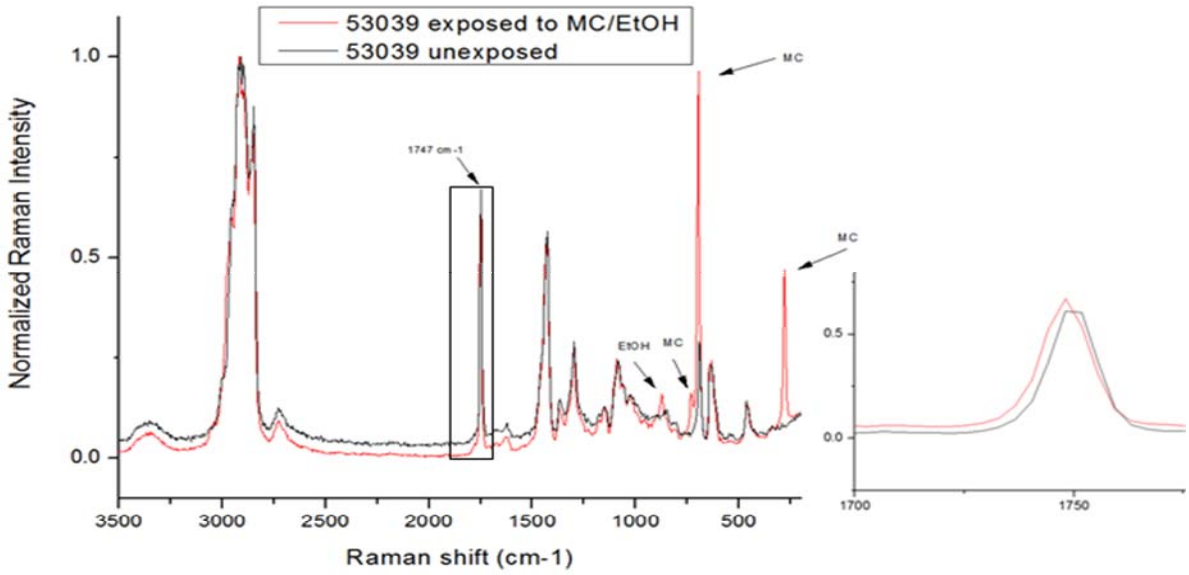

Figure 12. Raman spectra of MIL-53039 before and after exposure to methylene chloride and ethanol including an expansion to resolve the carbonyl peak.

Figure 13 shows the Raman spectroscopic result of the exposure of clearcoat MIL-53039 to a mixture of the solvents methylene chloride, ethanol, water and phenol. Here, phenol is the dominant solvent component visible in the spectra; methylene chloride is not visible. The most significant effect of this solvent is the reduction in intensity of the peaks corresponding to C=O (1750 cm^{-1}) and CH_2/CH_3 stretching (around 3000 cm^{-1}). This indicates a reduction in presence of these components but precise quantitative conclusions cannot be drawn from these results. There is also a small increase in the region of 1060 cm^{-1}, corresponding to C-O-C ether stretching.

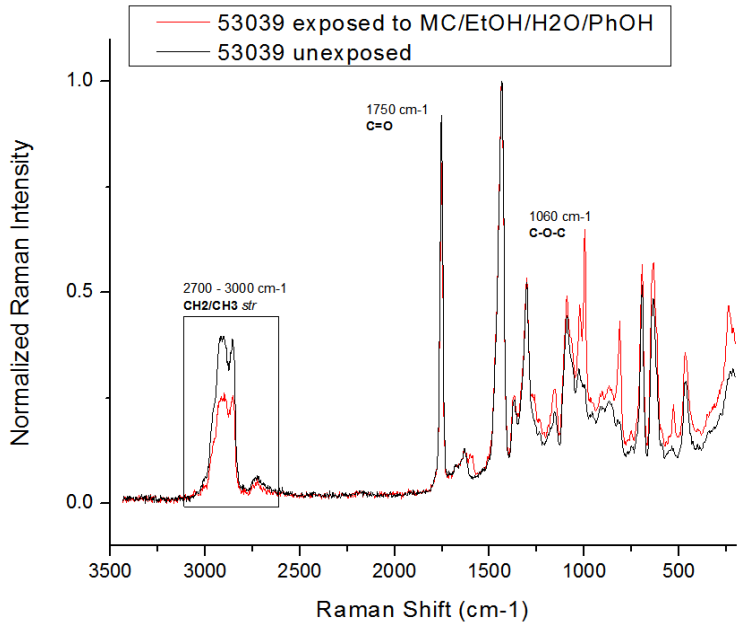

Figure 13. Raman spectra of MIL-53039 before and after exposure to a mixture of methylene chloride, ethanol, water and phenol.

The infrared spectrum of the same exposure, shown in Figure 14, provides even more interesting results. The peak representing C=O (around 1683 cm^{-1}) diminishes drastically, and a series of peaks indicative of ether C-O-C stretches (1167, 1152, 1117, 1069, 1025 and 1000 cm^{-1}) appear with moderate intensity. There is an obvious chemical change occurring.

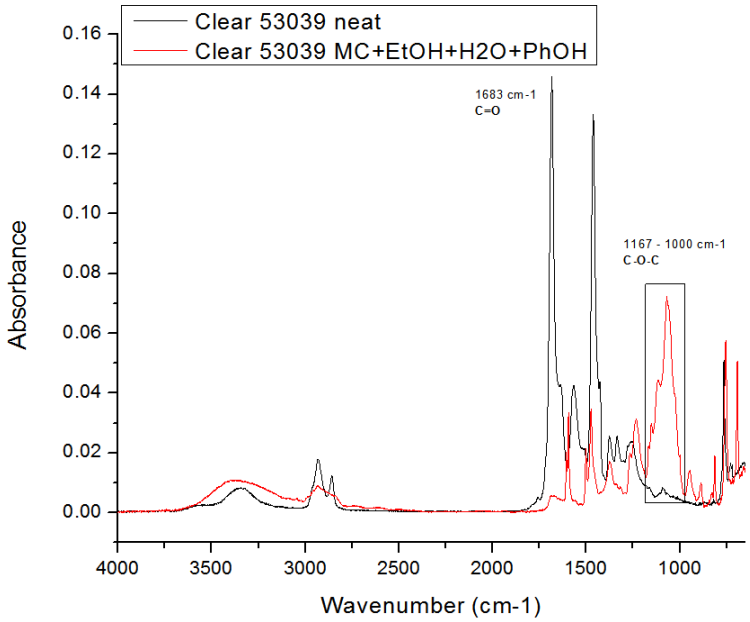

Figure 14. FTIR spectra of MIL-53039 before and after exposure to a mixture of methylene chloride, ethanol, water and phenol.

In light of the apparent effects of phenol, a separate experiment was performed to expose the MIL-53039 coating to liquid phenol (89 % PhOH, 11 % H_2O); the results are shown in Figure 15. Physically, the effects of this exposure are dramatic - the coating is dissolved into a shapeless mass within seconds of exposure. Even after several days of outgassing, significant quantities of phenol remain within the sample. There is significant reduction in peak intensity and area in the region around 3000 cm^{-1}, corresponding to CH_3 and CH_2 stretching modes, and at 1750 cm^{-1}, corresponding to C=O stretching; an increase is seen in the vicinity of expected ether stretches (1060 cm^{-1}) as well. Many likely regions for peak formation are overlapped by phenol vibrations, so peak deconvolution is problematic.

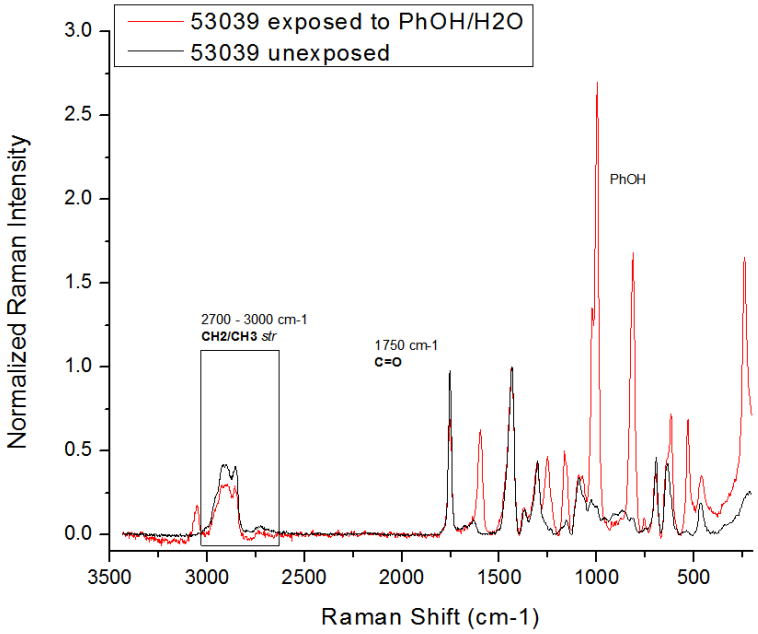

Figure 15. Raman spectra of MIL-53039 before and after exposure to phenol and water.

In order to obtain molecular level information about the effects of solvents upon clear coatings using a very different spectroscopic approach, solid-state proton (^1H) NMR spectroscopy was employed. The spectra and relaxation times (both T_1 and $T_{1\rho}$) of stationary (static) samples were obtained at 500 MHz (11.7 T field) on a Bruker DMX-500 NMR spectrometer in order to observe the effects of paint stripper components upon the segmental dynamics of the polymer chains, as well as the physical state of the solvent component(s). The spectra yield the full-linewidth at half-height (HHLW), which is decreased by segmental dynamics of polymer chain on time scales < 20 μs. The spin-lattice relaxation time T_1 is governed by fast dynamics on a ns

time scale (Fig 16). The spin-lattice relaxation time in the rotating frame ($T_{1\rho}$) is affected predominantly by slow motions (having a ~ 15 μs time scale), of the type that may permit solvent diffusion into polymer (Figure 16). By performing these measurements as a function of temperature, dynamics induced by a rise in temperature can be compared with dynamics induced by solvent swelling.

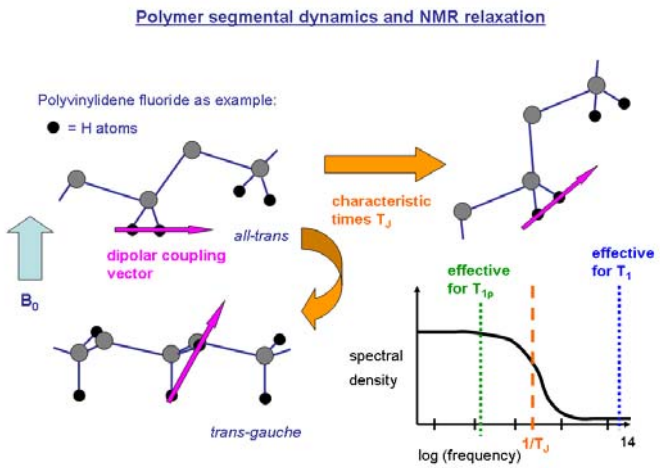

Figure 16. Schematic example of polymer segmental dynamics.

Figure 16 shows a schematic example of how polymer segmental dynamics (local conformational change in bottom molecule, longer-range reorientation of chain in top right molecule) modify the orientation of the internuclear proton-proton dipolar coupling vector with respect to the external magnetic field B_0. The resultant modulation of the dipolar coupling is responsible for NMR relaxation. The characteristic jump times involved, T_J, represent a correlation time for an assumed random process that can be related to a Lorentzian spectral density as shown in the log plot, with a cut-off frequency of $1/T_J$. For a dynamic process with the cut-off depicted, increasing temperature would raise the cut-off frequency while keeping the integrated spectral density constant, resulting in less-effective $T_{1\rho}$ relaxation (longer $T_{1\rho}$) and more-effective T_1 relaxation (shorter T_1).

The polyurethane topcoat clear film sample (MIL-DTL-53039) CARC was selected as the first sample to examine using the strategy described in the materials and methods section. The ^1H NMR results from the unexposed sample were compared with those from the same sample exposed to methylene chloride for 5 minutes. Figure 17 shows T_1 vs. temperature for the film before and after exposure to methylene chloride, as well as the T_1 for the neat solvent alone.

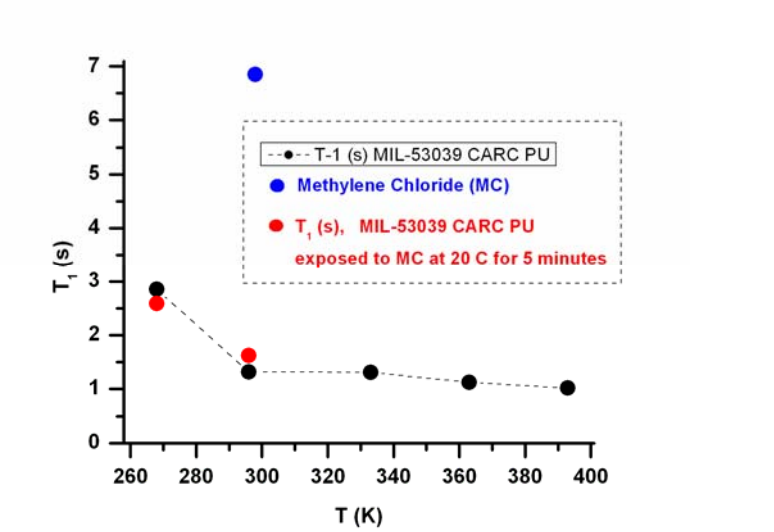

Figure 17. Proton NMR T_1 vs. temperature for MIL-DTL-53039 before and after 5-minute exposure to methylene chloride at 20 °C. Also shown is the T_1 of neat methylene chloride.

Several conclusions can be drawn from these data. The T_1 of neat methylene chloride is long because it is an isotropic liquid with a short (ns) rotational correlation time, whereas the T_1 of the unexposed polymer film is significantly shorter and typical of non-rigid polymers. The near-equality of the two T_1 values of the polyurethane sample exposed to methylene chloride to those in the starting polyurethane film at the same temperature indicates that methylene chloride is in intimate atomic-scale contact with the polymer, since the proton NMR signal from the methylene chloride component contributes to the overall spectrum of the exposed sample. This intimate contact results in the methylene chloride having significant proton-proton dipolar coupling to the polyurethane polymer, which equalizes T_1 values by the process known as spin-diffusion. There is no evidence whatsoever for free methylene chloride in liquid-like pools of any size, which would yield a sharper proton NMR peak having a longer T_1. Future experiments involving fully-formulated films having heterogeneous particles might show different behavior if delamination of interfaces occurs and allows methylene chloride to form small pools; the current experiments show how proton NMR can be used to observe such behavior.

In addition to these T_1 experiments on this same polyurethane film before and after exposure to methylene chloride, the $T_{1\rho}$ experiments as summarized in Figure 18 were conducted. The steep drop in $T_{1\rho}$ values for the unexposed film above the maximum around 330 K can be interpreted as due to the activation of relatively slow motions on a approximately 15 μs time scale (the

optimum for $T_{1\rho}$ relaxation at the rf field strength used, corresponding to a T_J of 15 μs in Figure 18).

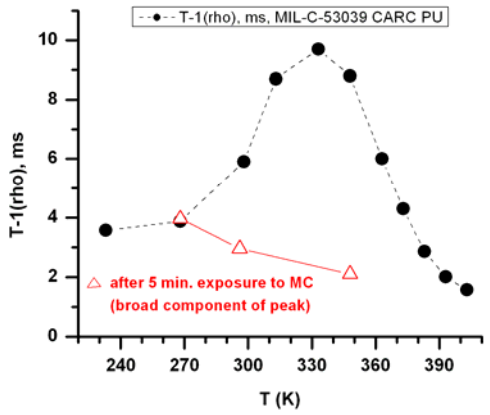

Figure 18. Proton NMR $T_{1\rho}$ vs. temperature for MIL-DTL-53039 film before and after 5-minute exposure to methylene chloride at 20 °C.

The proton NMR spectra of the CARC polyurethane topcoat (MIL-DTL-53039) clearcoat film are shown in Figure 19. The spectrum obtained at 296 K (23 °C) is greatly broadened by homonuclear dipolar interactions (ca. 50 kHz half-height linewidth), as expected for a crosslinked polymer with only limited segmental dynamics (the T_g measured above was 100 °C). Heating the sample to near the T_g (363 K, or 90 °C) results in a substantial reduction in the linewidth due to greatly increased segmental dynamics that partially average out the dipolar interactions.

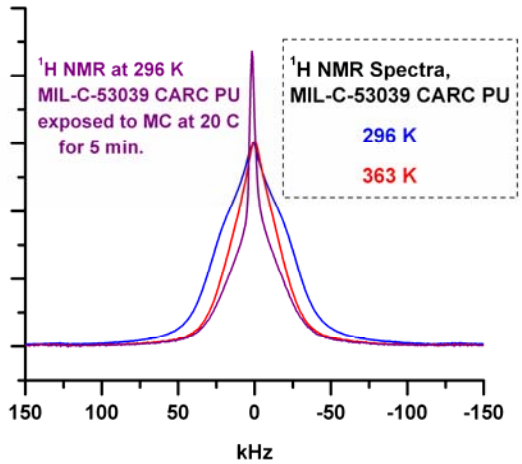

Figure 19. Wideline proton NMR spectra of MIL-DTL-53039 at two different temperatures, and after exposure to methylene chloride.

Similarly, exposure to methylene chloride for 5 minutes at 20 °C results in a spectrum at 296 K that is greatly narrowed by an increase in the segmental dynamics, similar to the effects of increasing temperature alone. (The T_g reported above of this sample after 2 hours exposure to methylene chloride was 67 °C.) The lineshape also has the appearance of a sharper and a broader component, the former of which is still broader than would be the case for purely liquid-like pools of methylene chloride. It is reasonable to attribute the sharper component to methylene chloride that is so strongly dipolar-coupled to nearby polymer protons that it shares the same T_1 relaxation time (Figure 19).

A similar NMR strategy was used to investigate the epoxy (polyamide) primer MIL-PRF-23377 clearcoat film, whose T_g of 40 °C reported above is much lower than that of the polyurethane topcoat (100 °C). The ^{1}H NMR half-height linewidths as a function of temperature are shown in Figure 20. The solvent proton NMR signals did not appear as sharp peaks that would be the case for liquid-like pools, but instead as broadened indistinct features in the spectrum. Because they represent a minor proton-containing component in the exposed sample, their contribution to the linewidth can be neglected to a first approximation. It is interesting to note that although the polyurethane and the epoxy polymers do not have the same chemical structure, the effective number density of their hydrogen atoms may be comparable, which in turn would yield comparable ^{1}H NMR linewidths for both in the rigid lattice limit (at low temperatures). Consequently, the approximately 50 kHz HHLW of the polyurethane film at 296 K is consistent with the fact that for the epoxy this broad linewidth is achieved only at approximately 230 K (-43 °C), which in both cases is about 80 °C below the respective T_g values.

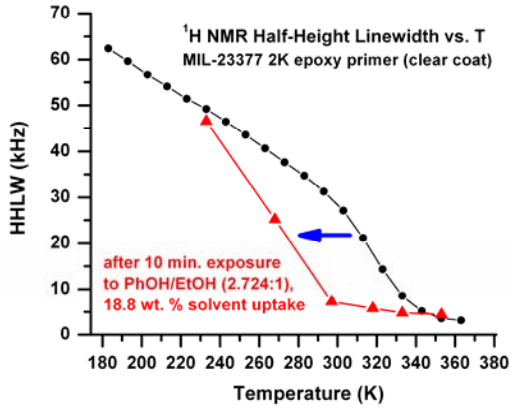

Figure 20. Proton NMR half-height linewidths vs. temperature for MIL-PRF-23377 before and after exposure to phenol/ethanol.

The effect of a 10-minute exposure to a phenol/ethanol mixture (2.7:1), which resulted in a 18.8 wt. % solvent uptake, upon the linewidth vs. temperature is also shown in Figure 20. The solvent exposure has markedly shifted the temperature at which a marked decrease in linewidth occurs, by roughly 40 °C. A somewhat larger decrease in the T_g, by 59 °C, was observed by DSC after a two hour exposure to the same solvent mixture. It is clear that this solvent combination alone can significantly affect segmental dynamics of the epoxy clearcoat film even after a short 10-minute exposure.

The ^{1}H $T_{1\rho}$ relaxation time vs. temperature for this same epoxy clearcoat film before and after a 10 minute exposure at 20 °C to the same phenol and ethanol mixture (2.7:1) is shown in Figure 21.

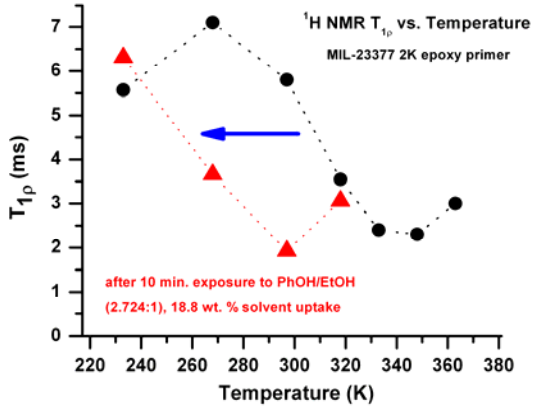

Figure 21. Proton NMR $T_{1\rho}$ relaxation times for MIL-PRF-23377 vs. temperature, before and after exposure to phenol/ethanol for 10 minutes at 20 °C.

Several points are worth noting. For the unexposed film, a clear minimum in $T_{1\rho}$ is observed at approximately 340 K (67 °C). As discussed above for the $T_{1\rho}$ results on the polyurethane film, this implies that slow segmental dynamics on a (T_J) time scale of 15 μs have their maximum spectral density at this temperature. In other words, segmental dynamics occurring at a rate of 70 kHz are activated and maximized when the temperature is raised to 340 K, which is some 27 °C above the measured T_g. The relationship deduced between the segmental dynamics associated with the polymer glass transition and the measured $T_{1\rho}$ values is supported by the (slightly extrapolated) $T_{1\rho}$ minimum for the polyurethane topcoat film at approximately 410 K in Figure 18, which would correspond to 37 °C above its T_g.

The effect of exposure to the phenol and ethanol solution upon the temperature dependence of $T_{1\rho}$ shown in Figure 21 is to shift the curve roughly 50 °C towards lower temperature. This results from the increased polymer segmental dynamics after solvent exposure, and is consistent with the similar shift of approximately 40 °C noted above for the linewidths.

Whether the increased segmental dynamics of the epoxy primer upon exposure to phenol/ethanol is due to a plasticization effect of solvent swelling, or instead to chemical attack and disruption of cross-links, is not assessed by these experiments. Solid-state ^2H NMR of deuterated phenol in this system should be able to substantiate IR evidence of chemical attack by phenol resulting in covalent bond formation to the polymer.

Conclusions to Date

We report here the creation of clear versions of currently in-use military coatings as well as their changes in physical and molecular-level properties after exposure to components of the paint stripper including methylene chloride and phenol. The coatings produced are polyurethane topcoats and epoxy primers and are similar to coatings in current military use. Casting the clear versions of the polyurethane formulas without imperfections was unsuccessful. Spray application of the clear films in many thin layers after substantial modifications to the original formulations from the original pigmented coatings systems proved to be the most successful method for producing a relatively defect free film. Antifoaming agents and flow modifiers were added without changing binder ratios; solvents known to be contained in the resin solutions and which stood alone in the original formula were added after substantially altering the solvent ratios to

achieve good film forming results by spray application. We characterize the coatings using DSC, TGA, FTIR-ATR and ^{1}H solid-state NMR. DSC shows significant depression of the glass transition temperature of all the coatings after exposure to solvent mixtures containing phenol, but little change after exposure to methylene chloride. The control mixture containing multiple solvents from the paint stripper caused the greatest coating degradation, suggesting that while phenol is the principal agent in glass transition depression, the other solvents play a significant role. TGA curves show greater weight loss at lower temperatures for coatings exposed to phenol. Findings from vibrational spectroscopy have indicated a significant change in the chemical structures as a result of solvent exposure. This change is particular to the solvent mixture used, especially phenol exposure, which causes the greatest difference in the spectra. Solid-state ^{1}H NMR data suggest that the stripper components rapidly exert very significant effects that increase the polymer segmental dynamics in a fashion similar to what takes place in the untreated coatings by heating to much higher temperatures. The data thus far suggest that there is a combination of chemical reaction of the most vulnerable linkages within the coating as well as destruction due to swelling beyond the capability of the polymer making up the coating. Additional studies are underway to prove this occurrence, as well as to further this observation to the fully formulated coating systems. The possibility of mechanically-induced covalent bond breakage due to swelling forces needs to be considered as our observations tend to support this idea. Likewise, the correlation of mechanism observed to other chemical substitutes is underway, which will lead to a better understanding and confirmation of the mode of action.

Literature Cited

Watson, K.E.; Wynne, J.H. Yesinowski, J.P.; Young, C.N.; Clayton, C.R. “Role of Methylene Chloride and Phenol in Chemical Paint Strippers” 41st Annual ACS Mid-Atlantic Regional Meeting, April 11, 2010; paper 212.

---

[i] Image from Cytec webpage, www.cytec.com